ChemPubSoc Europe

DOI: 10.1002/chem.201800596

CHEMISTRY A European Journal Communication

Solar Cells

Subnaphthalocyanines as Electron Acceptors in Polymer Solar Cells: Improving Device Performance by Modifying Peripheral and Axial Substituents

Chunhui Duan[+],*[a, b] David Guzmán[+],[c, d] Fallon J. M. Colberts,[b] René A. J. Janssen,*[b] and Tomás Torres*[c, d, e]

Abstract: A new class of subnaphthalocyanines bearing various peripheral and axial substituents have been synthesized for use as electron acceptors in solution-processed bulk-heterojunction polymer solar cells. The resulting solar cells exhibit modest photovoltaic performance with contributions from both the polymer donor and subnaphthalocyanine acceptor to the photocurrent.

Bulk-heterojunction (BHJ) polymer solar cells (PSCs) hold great promise as the next-generation photovoltaic technology due to their advantages, such as low-cost, flexibility, and compatibility with roll-to-roll processing and inkjet printing.[1] Recently, tremendous progress has been achieved in this field with power conversion efficiencies (PCEs) in excess of 12%.[2] In a BHJ-PSC, the core component is the active layer, in which the blend of an electron–donor and an electron–acceptor forms a phase separated morphology with a bicontinuous interpenetrating network. Although numerous electron donors including both conjugated polymers and small molecules have been extensively invented by chemists,[3] the electron acceptors were dominated by fullerene derivatives in the past two decades.[4] However, fullerene-based acceptors possess a few limitations, such as difficulty in synthesis and purification, low absorption coefficients, limited variability in the energy levels, and poor morphological stability in BHJ films.[5] Encouragingly, efficient non-fullerene acceptors have been developed in recent years that can overcome the shortcomings associated with fullerene-based acceptors.[5] The state-of-the-art PSCs built on non-fullerene acceptors produced remarkable PCEs over 13% in both single- and multi-junction devices, outperforming fullerene-based acceptors.[2b,c]

Despite many different n-type materials that were developed and assessed as acceptors in PSCs, two families of small molecular non-fullerene acceptors presently reach PCEs over 10% when blended with conjugated polymers. These are derivatives of aromatic diimide[6] and acceptor–donor–acceptor (A–D–A) type molecules with large central fused rings.[7] Nevertheless, the development of new non-fullerene acceptors beyond aromatic diimides and A–D–A molecules are also highly desired and may offer new properties.[8] Recently, we and other groups demonstrated that subphthalocyanines (SubPcs) are promising non-fullerene acceptors for PSCs.[9] SubPcs are aromatic chromophoric molecules with a boron at their inner cavity, a cone-shaped structure, and electron-transporting characteristics.[10] These characteristics render SubPcs good electron acceptor property and solution processability. By using PTB7-Th as the electron donor, solar cells with a PCE up to 4% and an external quantum efficiency (EQE) approaching 60% have been achieved by a SubPc derivative with chlorine atom as both peripheral and axial substituent (SubPc-Cl_6-Cl).[9a]

Subnaphthalocyanines (SubNcs) are similar to SubPcs, but offer extended conjugation in the peripheral cone of the molecule, becoming an important family of chromophores that exhibit outstanding photophysical properties showing strong electronic absorption and high fluorescence quantum yields.[11] Historically, SubNcs have been used as electron acceptors in vacuum-evaporated solar cells, reaching an impressive PCE of 8.4%.[12] However, SubNcs have never been tested as either

[a] Prof. C. Duan[+]
State Key Laboratory of Luminescent Materials and Devices, Institute of Polymer Optoelectronic Materials and Devices
South China University of Technology
Guangzhou 510640 (P.R. China)
E-mail: duanchunhui@scut.edu.cn

[b] Prof. C. Duan,[+] F. J. M. Colberts, Prof. R. A. J. Janssen
Molecular Materials and Nanosystems
Institute for Complex Molecular Systems
Eindhoven University of Technology
P. O. Box 513, 5600 MB Eindhoven (The Netherlands)
E-mail: r.a.j.janssen@tue.nl

[c] D. Guzmán,[+] Prof. T. Torres
Department of Organic Chemistry
Universidad Autónoma de Madrid
c/Francisco TomásyValiente 7, Cantoblanco, 28049 Madrid (Spain)
E-mail: tomas.torres@uam.es

[d] D. Guzmán,[+] Prof. T. Torres
Instituto Madrileño de Estudios Avanzados (IMDEA)-Nanociencia
c/Faraday, 9, Cantoblanco, 28049 Madrid (Spain)

[e] Prof. T. Torres
Institute for Advanced Research in Chemical Sciences (IAdChem)
UAM, 28049 Madrid (Spain)

[+] These authors contributed equally to this work.

Supporting information and the ORCID identification number(s) for the author(s) of this article can be found under: https://doi.org/10.1002/chem.201800596.

donors or acceptors in solution-processed BHJ solar cells. Herein, we report five SubNcs bearing different peripheral and axial substituents as electron acceptors in BHJ solar cells for the first time. Through the modification of the peripheral and axial substituents, the energy levels and the aggregation and crystallization behavior, and consequently, the photovoltaic device performance of the molecule can be tuned. A maximum PCE of 1.09% has been achieved for SubNc-F_{12}-OPh^{t}Bu demonstrating the ability of SubNcs to act as electron acceptor in BHJ PSC. This work paves the way to a new family of non-fullerene acceptors for BHJ PSCs through rational molecular modification.

The structure of the new SubNcs is shown in Scheme 1. The motivation for the design of these molecules starts from SubPc-Cl_6-Cl, which is our previously developed successful SubPc-based acceptor.[9a] The related SubNc is SubNc-Cl_{12}-Cl, which has the same peripheral and axial substituents. More peripheral chlorine atoms were introduced onto SubNc-Cl_{12}-Cl to downshift the lowest unoccupied molecular orbital (LUMO) level and to obtain acceptor character.

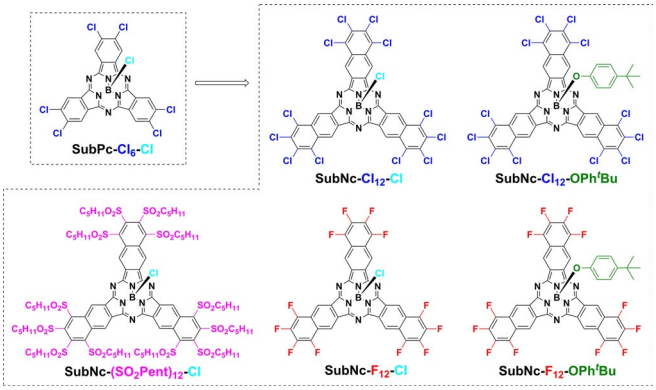

Scheme 1. Chemical structures of the SubNc derivatives studied in this work.

Following up on SubNc-Cl_{12}-Cl, another two SubNcs were synthesized by cyclotrimerization reaction of appropriate naphthalene-2,3-dicarbonitrile precursors, namely, SubNc-$(SO_2Pent)_{12}$-Cl and SubNc-F_{12}-Cl. Axial substitution of the corresponding SubNc-triflate derivative by reaction with *tert*-butylphenol afforded SubNc-Cl_{12}-OPh^{t}Bu and SubNc-F_{12}-OPh^{t}Bu, respectively. The synthetic procedures are shown in the Supporting Information. The solubility of the parent SubNc-Cl_{12}-Cl derivative is extremely poor in organic solvents, and hence, further characterizations were performed only on the other four SubNcs. X-ray diffraction analysis unequivocally determined the structure of SubNc-F_{12}-Cl, confirming the cone-shape structure characteristic of the subporphyrinoid family, as well as its tendency to build a columnar stacking organization (Figure 1, see the Supporting Information, selected crystallographic data).

The optical absorption spectra of the SubNcs in films and in solutions are shown in Figure 2a and Figure S4 (see the Supporting Information), respectively. SubNc-F_{12}-Cl and SubNc-F_{12}-OPh^{t}Bu exhibit very similar absorption profiles, indicating a

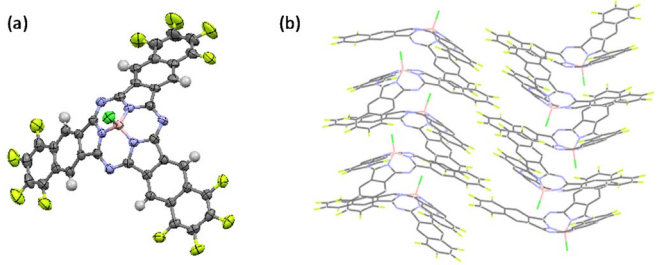

Figure 1. X-ray crystal structure of SubNc-F_{12}-Cl (CCDC 1583669 contains the supplementary crystallographic data for this paper. These data are provided free of charge by The Cambridge Crystallographic Data Centre). (a) Molecular structure showing thermal ellipsoids at the 50% probability level. (b) Columns packing along the *b* axis.

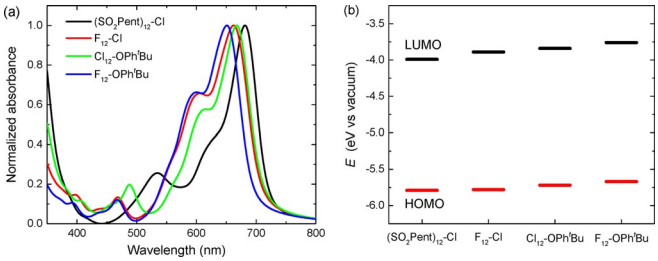

Figure 2. SubNcs: (a) optical absorption spectra of their films. (b) Their energy levels.

small influence of the axial substituent. More pronounced fluctuations in absorption spectra were observed when the peripheral substituents were changed, as was evidenced by the differences between SubNc-F_{12}-Cl and SubNc-$(SO_2Pent)_{12}$-Cl, and between SubNc-F_{12}-OPh^{t}Bu and SubNc-Cl_{12}-OPh^{t}Bu. In particular, SubNc-$(SO_2Pent)_{12}$-Cl shows the most redshifted absorption among all SubNcs. This indicates that the electronic coupling of the peripheral substituent to the SubNc framework is stronger than that of the axial substituent. Overall, SubNcs have redshifted and broader absorption compared to SubPcs, which can contribute to more efficient light absorption in solar cells.[9a] The fluorescence quantum yields (φ_F) were also measured in toluene,[11c] being around 0.20–0.30. The similitude of these values with the reported by Bender et al. suggest a same photoelectronic behavior of SubNcs.[12c] Notably, SubNcs exhibit a lower φ_F than SubPcs, suggesting shorter exciton lifetimes for SubNcs.[9a] Electrochemical properties and frontier orbital levels of the SubNcs were studied by cyclic voltammetry (CV) in tetrahydrofuran (THF). The CV data are presented in Figure S6 (see the Supporting Information) and the relevant frontier orbital energy levels are collected in Figure 2b and summarized in Table 1. The LUMO and highest occupied molecular orbital (HOMO) energy levels were estimated from the reduction potentials obtained by CV measurements and optical band gap (E_g) values. Interestingly, the axial substituent has important influence on both the LUMO and HOMO levels of the SubNcs, whereas the peripheral substituents exert only significant influence on the LUMO levels but not on the HOMO levels of the SubNcs. For example, changing the axial substituent from SubNc-F_{12}-Cl to SubNc-F_{12}-OPh^{t}Bu results in a consid-

Table 1. Optical properties and energy levels of the SubNcs.

SubNc-X	λ_{max} [nm]		E_g^{opt} [eV]	HOMO [eV]	LUMO [eV]	φ_F
	solution	film				
$(SO_2Pent)_{12}$-Cl	677	682	1.80	−5.79	−3.99	0.297
F_{12}-Cl	646	662	1.89	−5.78	−3.89	0.214
Cl_{12}-OPh^{t}Bu	644	666	1.88	−5.72	−3.84	0.242
F_{12}-OPh^{t}Bu	640	650	1.91	−5.67	−3.76	0.218

erable up-shifting (>0.1 eV) of both LUMO and HOMO levels. On the contrary, the change of peripheral substituent (SubNc-F_{12}-Cl versus SubNc-$(SO_2Pent)_{12}$-Cl, and SubNc-F_{12}-OPh^{t}Bu versus SubNc-Cl_{12}-OPh^{t}Bu) cause about 0.1 eV fluctuation of LUMO levels but a much smaller fluctuation of HOMO levels. Nevertheless, all SubNcs possess deep-lying LUMO levels (below −3.76 eV), endowing them with electron-accepting character.

The photovoltaic properties of the SubNcs acceptors were evaluated in solar cells in combination with PTB7-Th as a low-band-gap donor polymer in an ITO/ZnO/PTB7-Th:SubNc-X/MoO_x/Ag device structure under simulated air mass 1.5 global (AM1.5G) illumination (100 mW cm^{-2}). Integration of the external quantum efficiency (EQE) with the AM1.5G spectrum was used to accurately determine the short-circuit current density and calculate the PCE of the solar cells. The current density/voltage (*J*/*V*) curves and EQE spectra of the optimized devices are shown in Figure 3, and Table 2 summarizes the photovoltaic parameters. Device statistics can be found in Table S2 (see the Supporting Information). Results from different fabricating conditions are presented in Table S1. The highest PCE of 1.09% was found for SubNc-F_{12}-OPh^{t}Bu, along with a short-circuit current density (J_{sc}) of 3.9 mA cm^{-2}, an open-circuit voltage (V_{oc}) of 0.73 V, and a fill factor (FF) of 0.38. The V_{oc} provided by SubNc-F_{12}-OPh^{t}Bu is only slightly less than for PTB7-Th:fullerene devices (about 0.8 V), but the V_{oc} of the solar cells based on other SubNcs with PTB7-Th is lower due to their deeper LUMO levels.[13] As shown in Figure 3b, both the polymer donor and the SubNc acceptor contribute to the photocurrent in each case. Except for SubNc-$(SO_2Pent)_{12}$-Cl, absorption spectra of which has substantial overlap with the donor polymer PTB7-Th, all other SubNcs exhibit a EQE maximum located at about 540 nm and EQE shoulder located at about 710 nm, which originate from the SubNcs and PTB7-Th, respectively. Nevertheless, all these SubNcs gave relative low overall EQEs of ≤0.25 and thereby low J_{sc} values of <4 mA cm^{-2}. Another common limitation of these solar cells is their low FF (≤0.46), which is much lower than that of high-performing solar cells based on fullerene acceptors and A–D–A acceptors. As a result, all these devices show relative low PCE values. A low FF may result from space-charge limited photocurrent, when the mobilities for holes and electrons are largely unbalanced.[14] We thus focused on understanding the reason for the low J_{sc} and FF of the devices based on these SubNcs acceptors.

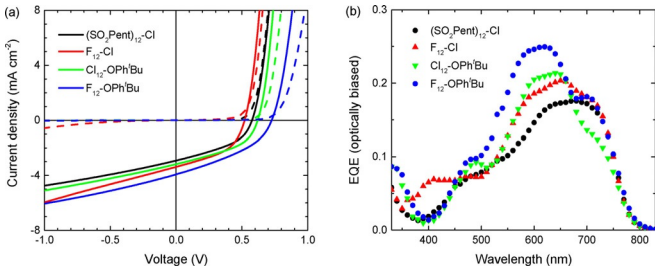

Figure 3. (a) *J*/*V* curves of the PTB7-Th:SubNc solar cells in dark (dashed lines) and under illumination (solid lines). (b) Corresponding EQE spectra.

Table 2. Solar cell characteristics and charge carrier mobilities of PTB7-Th:SubNc devices.

SubNc-X	J_{sc}[a] [mA cm^{-2}]	V_{oc} [V]	FF	PCE [%]	EQE_{max}
$(SO_2Pent)_{12}$-Cl	2.9	0.58	0.42	0.71	0.18
F_{12}-Cl	3.4	0.52	0.46	0.82	0.20
Cl_{12}-OPh^{t}Bu	3.2	0.62	0.44	0.86	0.21
F_{12}-OPh^{t}Bu	3.9	0.73	0.38	1.09	0.25

[a] Determined by integrating the EQE spectrum with the AM1.5G spectrum.

The transport and recombination of charge carriers in the blend films of PTB7-Th:SubNc were investigated. Hole mobilities (μ_h) and electron mobilities (μ_e; Table S3 in the Supporting Information) were estimated from single-carrier PTB7-Th:SubNc devices by fitting the *J*–*V* data (Figure S7 in the Supporting Information) to a space-charge-limited current model, resulting in a $\mu_h \approx 10^{-4}$ and a $\mu_e \approx 10^{-6}$ cm^2 V^{-1} s^{-1} for all four acceptors. Bearing in mind that both the μ_h and μ_e of PTB7-Th:fullerene blends are usually $\approx 10^{-3}$ cm^2 V^{-1} s^{-1}, the greatly reduced electron-transport capability of the PTB7-Th:SubNc films is likely causing the low J_{sc} and low FF. Moreover, the transport of hole and electron in these films is highly imbalanced as suggested by the high μ_h/μ_e value of >100 for all SubNc-based acceptors. The build-up of space charge due to the imbalanced hole/electron transport further increased the possibility of bimolecular charge recombination, an important factor resulting in photocurrent loss and poor FF. The strong bimolecular recombination was further evidenced by the large difference between the EQE measured with light bias (EQE_{bias}) and without light bias (EQE_{nobias}; Figure S8 in the Supporting Information). The average values for $\rho = EQE_{bias}/EQE_{nobias}$ (Figure 4) can be used to evaluate the bimolecular recombination efficiency through $\eta_{BR} = 1-\rho$.[15] Clearly, the low ρ values indicate substantial bimolecular recombination. State-of-the-art PSCs often show a ρ value approaching unity. The ρ values of these PTB7-Th:SubNc solar cells are all lower than 0.85, suggesting significant bimolecular recombination losses, even at short circuit. The extensive bimolecular recombination in the maximum power point and at short circuit was also evidenced by the steady increase of current density of illuminated solar cells under reverse bias (Figure 3a), in which the enhanced electric field promotes transport of the slowest carriers. The fact that the dark current does not increase to the same extent under reverse bias excludes the possibility that the increased current density under illumination is due to a low shunt resistance. Such behavior is

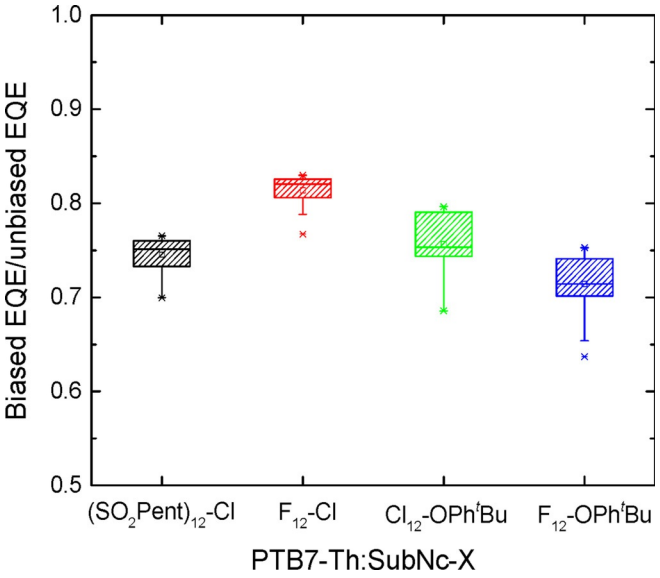

Figure 4. Average EQE_{bias}/EQE_{nobias} values of PTB7-Th:SubNc solar cells.

often found in bulk-heterojunction blends with an intimately mixed morphology and one slow carrier.[16]

The morphology of PTB7-Th:SubNc blend films was studied by transmission electron microscopy (TEM). In TEM data, all PTB7-Th:SubNc blends exhibit rather homogeneous films without noteworthy phase separation (Figure 5). In such intimately mixed blends, charge separation is impeded because of the lack of pure domains. It is well recognized that pure domains promote charge dissociation from the donor/acceptor interface, whereas impure domain often results in serious geminate recombination.[17] Moreover, charge transport is blocked in such intimately mixed blends due to lack of continuous pathways for the transport of the photogenerated charge carriers, causing accumulation of space charge and recombination losses. Collectively, the low-charge mobility, imbalanced hole/electron transport, and the suboptimal BHJ morphology are factors that contribute to recombination losses and that limit the J_{sc} and FF of PTB7-Th:SubNc solar cells.

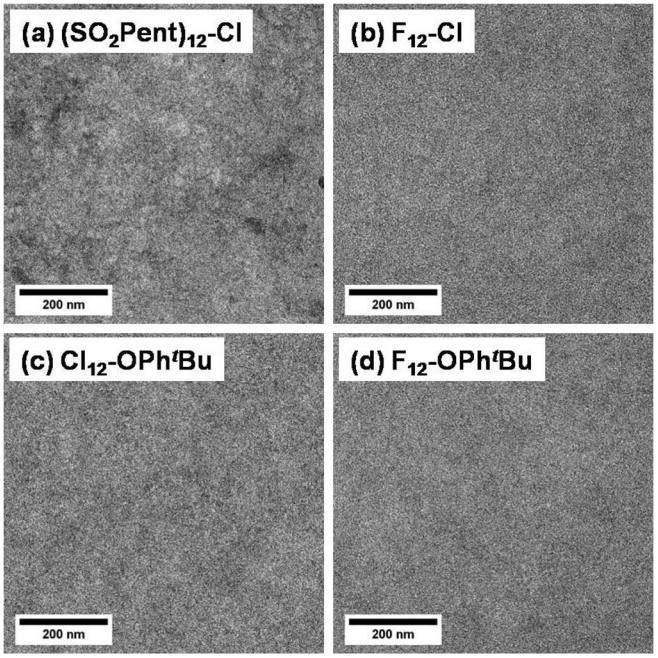

Figure 5. Bright-field TEM images of the PTB7-Th:SubNc blend films deposited with the same methods as those for PSC fabrication. Scale bar: 200 nm.

Notably, the highest PCE of SubNcs is much lower than that of our previously reported successful acceptor SubPc-Cl_6-Cl (1.09% versus 4.0%).[9a] This can be rationalized considering the following aspects. First, SubPc-Cl_6-Cl has a small chlorine atom in the axial position, whereas SubNc-F_{12}-OPh^{t}Bu, which provided the best solar cells, has a bulky OPh^{t}Bu group in the axial position. The small axial chlorine atom favors the formation of head-to-tail columnar stacks and thus prompts charge transport, whereas the bulky OPh^{t}Bu group precludes this behavior and thus deteriorates charge transport.[9a] Second, the shorter exciton lifetimes of SubNcs compared to SubPc-Cl_6-Cl as suggested by the lower fluorescence quantum yields is limiting the fraction of excitons that reach the donor/acceptor interface, in which the exciton dissociates, reducing the EQEs of the SubNcs-based solar cells. Third, the SubNcs show redshifted absorption spectra with respect to SubPcs,[9a] which have a considerable spectral overlap between SubNcs and the polymer donor PTB7-Th.

In conclusion, boron subnaphthalocyanines bearing different peripheral and axial substituents have been synthesized and utilized as electron acceptors in BHJ polymer solar cells for the first time. Due to their acceptor character, their blends with PTB7-Th, a narrow band gap conjugated polymer, exhibit photovoltaic performance with contributions from both the polymer donor and the SubNc acceptor to the photocurrent. Nevertheless, the highest PCE of the SubNc-based solar cells is only 1.09%. The main limitations of these SubNc-based solar cells is their low J_{sc} and FF, which is a combined result of low charge mobility, imbalanced hole/electron transport, and a suboptimal BHJ morphology contributing to recombination losses. Therefore, the future research involving subnaphthalocyanines should focus on improving electron mobility, and controlling morphology of the blends to avoid geminate recombination and reduce bimolecular recombination losses.

Acknowledgements

The work was performed in the framework of the Mujulima (EU-FP7, No. 604148) and Triple Solar (ERC Adv Grant No. 339031) projects, and received funding from the Ministry of Education, Culture and Science of Netherlands (Gravity program 024.001.035). We are also grateful to MINECO, Spain (CTQ2014-52869-P) and the Comunidad de Madrid, Spain (FOTOCARBON, S2013/MIT-2841). The research was also financially supported by the Startup Fund for Distinguished Scholars of SCUT (j2rs-K5173590). D.G. acknowledges Spanish MICINN for his F.P.I. fellowship.

Conflict of interest

The authors declare no conflict of interest.

Keywords: device performance · electron acceptors · polymer solar cells · subnaphthalocyanines · substituents

[1] a) G. Yu, J. Gao, J. C. Hummelen, F. Wudl, A. J. Heeger, *Science* **1995**, *270*, 1789 – 1791; b) F. C. Krebs, J. Fyenbo, M. Jorgensen, *J. Mater. Chem.* **2010**, *20*, 8994 – 9001; c) A. J. Heeger, *Adv. Mater.* **2014**, *26*, 10 – 28; d) L. Lu, T. Zheng, Q. Wu, A. M. Schneider, D. Zhao, L. Yu, *Chem. Rev.* **2015**, *115*, 12666 – 12731.

[2] a) M. Li, K. Gao, X. Wan, Q. Zhang, B. Kan, R. Xia, F. Liu, X. Yang, H. Feng, W. Ni, Y. Wang, J. Peng, H. Zhang, Z. Liang, H.-L. Yip, X. Peng, Y. Cao, Y. Chen, *Nat. Photonics* **2017**, *11*, 85 – 90; b) W. Zhao, S. Li, H. Yao, S. Zhang, Y. Zhang, B. Yang, J. Hou, *J. Am. Chem. Soc.* **2017**, *139*, 7148 – 7151; c) Y. Cui, H. Yao, B. Gao, Y. Qin, S. Zhang, B. Yang, C. He, B. Xu, J. Hou, *J. Am. Chem. Soc.* **2017**, *139*, 7302 – 7309.

[3] C. Duan, F. Huang, Y. Cao, *J. Mater. Chem.* **2012**, *22*, 10416 – 10434.

[4] a) J. C. Hummelen, B. W. Knight, F. LePeq, F. Wudl, J. Yao, C. L. Wilkins, *J. Org. Chem.* **1995**, *60*, 532 – 538; b) M. M. Wienk, J. M. Kroon, W. J. H. Verhees, J. Knol, J. C. Hummelen, P. A. van Hal, R. A. J. Janssen, *Angew. Chem. Int. Ed.* **2003**, *42*, 3371 – 3375; *Angew. Chem.* **2003**, *115*, 3493 – 3497.

[5] a) C. B. Nielsen, S. Holliday, H.-Y. Chen, S. J. Cryer, I. McCulloch, *Acc. Chem. Res.* **2015**, *48*, 2803 – 2812; b) Y. Duan, X. Xu, H. Yan, W. Wu, Z. Li, Q. Peng, *Adv. Mater.* **2017**, *29*, 1605115; c) G. J. Zhang, F. Yang, H. Yan, J.-H. Kim, H. Ade, W. Wu, X. Xu, Y. Duan, Q. Peng, *Adv. Mater.* **2017**, *29*, 1606054.

[6] a) Y. Zhong, M. T. Trinh, R. Chen, G. E. Purdum, P. P. Khlyabich, M. Sezen, S. Oh, H. Zhu, B. Fowler, B. Zhang, W. Wang, C.-Y. Nam, M. Y. Sfeir, C. T. Black, M. L. Steigerwald, Y.-L. Loo, F. Ng, X. Y. Zhu, C. Nuckolls, *Nat. Commun.* **2015**, *6*, 8242; b) D. Meng, H. Fu, C. Xiao, X. Meng, T. Winands, W. Ma, W. Wei, B. Fan, L. Huo, N. L. Doltsinis, Y. Li, Y. Sun, Z. Wang, *J. Am. Chem. Soc.* **2016**, *138*, 10184 – 10190; c) J. Yi, Y. Wang, Q. Luo, Y. Lin, H. Tan, H. Wang, C.-Q. Ma, *Chem. Commun.* **2016**, *52*, 1649 – 1652; d) J. Zhang, X. Zhang, G. Li, H. Xiao, W. Li, S. Xie, C. Li, Z. Bo, *Chem. Commun.* **2016**, *52*, 469 – 472; e) A. Zhang, C. Li, F. Yang, J. Zhang, Z. Wang, Z. Wei, W. Li, *Angew. Chem. Int. Ed.* **2017**, *56*, 2694 – 2698; *Angew. Chem.* **2017**, *129*, 2738 – 2742.

[7] a) Y. Lin, J. Wang, Z.-G. Zhang, H. Bai, Y. Li, D. Zhu, X. Zhan, *Adv. Mater.* **2015**, *27*, 1170 – 1174; b) S. Dai, F. Zhao, Q. Zhang, T.-K. Lau, T. Li, K. Liu, Q. Ling, C. Wang, X. Lu, W. You, X. Zhan, *J. Am. Chem. Soc.* **2017**, *139*, 1336 – 1343; c) S. Holliday, R. S. Ashraf, A. Wadsworth, D. Baran, S. A. Yousaf, C. B. Nielsen, C.-H. Tan, S. D. Dimitrov, Z. Shang, N. Gasparini, M. Alamoudi, F. Laquai, C. J. Brabec, A. Salleo, J. R. Durrant, I. McCulloch, *Nat. Commun.* **2016**, *7*, 11585; d) D. Baran, T. Kirchartz, S. Wheeler, S. Dimitrov, M. Abdelsamie, J. Gorman, R. S. Ashraf, S. Holliday, A. Wadsworth, N. Gasparini, P. Kaienburg, H. Yan, A. Amassian, C. J. Brabec, J. R. Durrant, I. McCulloch, *Energy Environ. Sci.* **2016**, *9*, 3783 – 3793.

[8] a) F. G. Brunetti, X. Gong, M. Tong, A. J. Heeger, F. Wudl, *Angew. Chem. Int. Ed.* **2010**, *49*, 532 – 536; *Angew. Chem.* **2010**, *122*, 542 – 546; b) Z. Mao, W. Senevirathna, J.-Y. Liao, J. Gu, S. V. Kesava, C. Guo, E. D. Gomez, G. Sauvé, *Adv. Mater.* **2014**, *26*, 6290 – 6294; c) A. N. Bartynski, M. Gruber, S. Das, S. Rangan, S. Mollinger, C. Trinh, S. E. Bradforth, K. Vandewal, A. Salleo, R. A. Bartynski, W. Bruetting, M. E. Thompson, *J. Am. Chem. Soc.* **2015**, *137*, 5397 – 5405.

[9] a) C. Duan, G. Zango, M. García Iglesias, F. J. M. Colberts, M. M. Wienk, M. V. Martínez-Díaz, R. A. J. Janssen, T. Torres, *Angew. Chem. Int. Ed.* **2017**, *56*, 148 – 152; *Angew. Chem.* **2017**, *129*, 154 – 158; b) B. Ebenhoch, N. B. A. Prasetya, V. M. Rotello, G. Cooke, I. D. W. Samuel, *J. Mater. Chem. A* **2015**, *3*, 7345 – 7352; c) D. S. Josey, S. R. Nyikos, R. K. Garner, A. Dovijarski, J. S. Castrucci, J. M. Wang, G. J. Evans, T. P. Bender, *ACS Energy Lett.* **2017**, *2*, 726 – 732; d) J. S. Castrucci, R. K. Garner, J. D. Dang, E. Thibau, Z.-H. Lu, T. P. Bender, *ACS Appl. Mater. Interfaces* **2016**, *8*, 24712 – 24721.

[10] a) C. G. Claessens, D. González-Rodríguez, M. S. Rodríguez-Morgade, A. Medina, T. Torres, *Chem. Rev.* **2014**, *114*, 2192 – 2277; b) J. Guilleme, M.-J. Mayoral, J. Calbo, J. Aragó, P. M. Viruela, E. Ortí, D. González-Rodríguez, T. Torres, *Angew. Chem. Int. Ed.* **2015**, *54*, 2543 – 2547; *Angew. Chem.* **2015**, *127*, 2573 – 2577; c) J. Guilleme, E. Cavero, T. Sierra, J. Ortega, C. L. Folcia, J. Etxebarria, T. Torres, D. González-Rodríguez, *Adv. Mater.* **2015**, *27*, 4280 – 4284; d) K. A. Winterfeld, G. Lavarda, J. Guilleme, M. Sekita, D. M. Guldi, T. Torres, G. Bottari, *J. Am. Chem. Soc.* **2017**, *139*, 5520 – 5529.

[11] a) M. Geyer, F. Plenzig, J. Rauschnabel, M. Hanack, B. Del Rey, A. Sastre, T. Torres, *Synthesis* **1996**, 1139 – 1151, https://doi.org/10.1055/s-1996 – 4349; b) N. Kobayashi, T. Ishizaki, K. Ishii, H. Konami, *J. Am. Chem. Soc.* **1999**, *121*, 9096 – 9110; c) S. Nonell, N. Rubio, B. del Rey, T. Torres, *J. Chem. Soc. Perkin Trans. 1* **2000**, *2*, 1091 – 1094; d) G. Martín, G. Rojo, F. Agulló-López, V. R. Ferro, J. M. García de la Vega, M. V. Martínez-Díaz, T. Torres, I. Ledoux, J. Zyss, *J. Phys. Chem. B* **2002**, *106*, 13139 – 11314; e) S. Shimizu, A. Miura, S. Khene, T. Nyokong, N. Kobayashi, *J. Am. Chem. Soc.* **2011**, *133*, 17322 – 17328.

[12] a) K. Cnops, B. P. Rand, D. Cheyns, B. Verreet, M. A. Empl, P. Heremans, *Nat. Commun.* **2014**, *5*, 3406; b) J. Endres, I. Pelczer, B. P. Rand, A. Kahn, *Chem. Mater.* **2016**, *28*, 794 – 801; c) J. D. Dang, D. S. Josey, A. J. Lough, Y. Li, A. Sifate, Z.-H. Lu, T. P. Bender, *J. Mater. Chem. A* **2016**, *4*, 9566 – 9577.

[13] M. C. Scharber, D. Mühlbacher, M. Koppe, P. Denk, C. Waldauf, A. J. Heeger, C. J. Brabec, *Adv. Mater.* **2006**, *18*, 789 – 794.

[14] V. D. Mihailetchi, J. Wildeman, P. W. M. Blom, *Phys. Rev. Lett.* **2005**, *94*, 126602.

[15] L. J. A. Koster, M. Kemerink, M. M. Wienk, K. Maturová, R. A. J. Janssen, *Adv. Mater.* **2011**, *23*, 1670 – 1674.

[16] D. Bartesaghi, M. Turbiez, L. J. A. Koster, *Org. Electron.* **2014**, *15*, 3191 – 3202.

[17] D. Veldman, O. İpek, S. C. J. Meskers, J. Sweelssen, M. M. Koetse, S. C. Veenstra, J. M. Kroon, S. S. v. Bavel, J. Loos, R. A. J. Janssen, *J. Am. Chem. Soc.* **2008**, *130*, 7721 – 7735.

Manuscript received: February 5, 2018
Revised manuscript received: February 28, 2018
Accepted manuscript online: March 9, 2018
Version of record online: April 10, 2018

